RAA 2021 Vol. **21** No. **11**, 283(8pp) doi: 10.1088/1674-4527/21/11/283

http://www.raa-journal.org *http://iopscience.iop.org/raa*

***R**esearch in*
***A**stronomy and*
***A**strophysics*

Multi-parameter identification of gratings measurement by Experimental Ray Tracing

Li-Si Chen[1,2,3], Zhong-Wen Hu[1,2], Hai-Jiao Jiang[1,2], Hui-Min Kang[1,2] and Chen-Zhong Wang[1,2,3]

[1] National Astronomical Observatories/Nanjing Institute of Astronomical Optics & Technology, Chinese Academy of Sciences, Nanjing 210042, China; *lschen@niaot.ac.cn*
[2] CAS Key Laboratory of Astronomical Optics & Technology, Nanjing Institute of Astronomical Optics & Technology, Nanjing 210042, China
[3] University of Chinese Academy of Sciences, Beijing 100049, China

Received 2021 January 24; accepted 2021 August 25

Abstract A simple method for measuring grating groove density as well as its position and orientation is proposed based on the idea of ERT (Experimental Ray Tracing). Conventional methods only measure grating groove density with accuracy limited by its rotary stage and goniometer. The method proposed in the paper utilizes linear guides which could be calibrated to much higher accuracy. It is applicable to gratings of arbitrary surface profile or mosaic of a group of various gratings. Various measurement error sources are simulated by the Monte Carlo method and the results show high accuracy capability of grating parameters identification. A verification testing is performed. The accuracy dependency on main configuration parameters is evaluated. A method to expand measurement range by double wavelength is also discussed.

Key words: grating — groove density — position — orientation — measurement range

1 INTRODUCTION

The methods to measure grating groove density include AFM (Sharma et al. 2012), interference method, Moire fringe method (Oster et al. 1964), LTP (Liu et al. 2006), and other diffraction method. The diffraction method is widely used owing to its simplicity by using either Littrow configuration (Wang et al. 2015; Du et al. 2016) or Littman configuration (Tai et al. 1999). The accuracy is limited by its rotary stage and goniometer used in conventional diffraction methods. Furthermore, it is necessary to place a grating sample exactly at the center of a rotating stage, or an off-center inducing error occurs for measurement. A few methods for correcting the error is given by data processing (Hiroyuki & Tomohiro 2014; Hu et al. 2004) or by improved setups (Wang et al. 2015; Sheng et al. 2017, 2018). Capability of conventional methods on measuring non-planar gratings or VLS (Varied Line Space) gratings is restricted. It is difficult to cover the measurement of mosaic of a group of gratings.

In this paper, a simple method is proposed to achieve grating multiple parameter identification simultaneously by drawing the ideas from ERT (Experimental Ray Tracing) (Häusler & Schneider 1988). By detecting a few diffracted ray directions which would be extracted from ray positions of parallel planes, grating groove density as well as its position and orientation relative to a reference plane is measured simultaneously. It is applicable to gratings of arbitrary surfaces or mosaic gratings and it utilizes linear guides which could be calibrated to much higher accuracy. It employs a single wavelength laser beam with fixed direction. Gratings under test would be kept stationary, thus measurement uncertainty is only from linear guides and the image centroid algorithm which could well be traced. The Monte Carlo method is used to simulate measurement accuracy.

2 THE PRINCIPLE OF ERT ON GRATING MEASUREMENT

ERT is widely used in profiler metrology of conventional optical components. It proves its abilities in numerous optical components surface profile measurement (Ceyhan et al. 2011; Gutierrez et al. 2017; Binkele et al. 2018b, 2017, 2018a). When a ray incidents on an optical component, the direction of transmitted or reflected rays can be determined. This direction gives information about the optical component at the investigated position based on ERT. We propose a method in grating multiple parameter

identification instead, the directions of a few diffracted lights are measured, then grating parameters are obtained by grating equation as well as its position and orientation.

The sketch of testing system includes a laser source, a 2D translation stage, and a CCD detector, as shown in Figure 1. Gratings under test could be either reflection gratings or transmission gratings since they both have diffract rays by the reflection side. The detector is situated on the 2D translation stage. It shifts vertically and obtains ray hit point image among different parallel planes. In order to cover possible ray extent, the detector should move horizontally. A unified coordinate system is assumed: the reference plane (horizontal plane) as the xOy plane, the z axis is perpendicular to the xOy plane.

2.1 Calibration Accuracy of the Translation Stage Tilt

All the testing system components should be calibrated before measurement. Here the detector shifting vertically and obtains ray hit point image on CCD or CMOS detector among different parallel planes. The vertical arm of the 2D translation table must be straight down (parallel to the z-axis), the tilt angle of the vertical arm relative to z-axis is called verticality in the paper. The tilt angle of the horizontal arm relative to xOy is called horizontality. They are less than $60''$ after calibrating.

2.2 Multi-parameter Identification of Grating

This section introduces the grating parameter identification. The experimental steps are as follows: Firstly, the grating sample must be carefully aligned and keeps stationary. The narrow laser beam introduces into the grating vertically with a fixed direction perpendicular to the xOy plane as Figure 1.

Secondly, CCD shifts vertically in two different height planes with the height h_1 and h_2 from the reference plane respectively. It is assumed that the distance between the two planes is h with $h = h_1 - h_2$. Then CCD obtains ray hit point image among the two planes and records the position of the rays. The detector should move horizontally to cover possible ray extent. The centroid of the +1-order, 0-order and –1-order diffracted ray on the first plane are denoted as $A_{1,1}$, $A_{1,0}$ and $A_{1,-1}$ with the coordinate $(x_{1,1}, y_{1,1}, h_1)$, $(x_{1,0}, y_{1,0}, h_1)$ and $(x_{1,-1}, y_{1,-1}, h_1)$, respectively. Move down the CCD to the second plane. The centroid of the +1-order, 0-order and –1-order diffracted ray on the second plane are denoted as $A_{2,1}$, $A_{2,0}$ and $A_{2,-1}$ with the coordinate $(x_{2,1}, y_{2,1}, h_2)$, $(x_{2,0}, y_{2,0}, h_2)$ and $(x_{2,-1}, y_{2,-1}, h_2)$, respectively.

Thirdly, two internal angles between 0-order ray and +1-order or –1-order ray are obtained according above six points. The cosine of the angle between the +1-order diffracted ray and the 0-order ray is denoted as t. The cosine of the angle between the –1-order diffracted ray and the 0-order ray is denoted as l. They satisfy

$$\begin{aligned} t &= \frac{|(x_{1,1}-x_{2,1})(x_{1,0}-x_{2,0})+(y_{1,1}-y_{2,1})(y_{1,0}-y_{2,0})+h^2|}{\sqrt{(x_{1,1}-x_{2,1})^2+(y_{1,1}-y_{2,1})^2+h^2}*\sqrt{(x_{1,0}-x_{2,0})^2+(y_{1,0}-y_{2,0})^2+h^2}}\,, \\ l &= \frac{|(x_{1,-1}-x_{2,-1})(x_{1,0}-x_{2,0})+(y_{1,-1}-y_{2,-1})(y_{1,0}-y_{2,0})+h^2|}{\sqrt{(x_{1,-1}-x_{2,-1})^2+(y_{1,-1}-y_{2,-1})^2+h^2}*\sqrt{(x_{1,0}-x_{2,0})^2+(y_{1,0}-y_{2,0})^2+h^2}}\,. \end{aligned} \tag{1}$$

Lastly, the grating parameters can be obtained from the grating equation and the two internal angles. If the grating works in azimuth angle $\gamma = 0$. Here, for a given wavelength λ, the grating incident angle θ, the m-order diffraction angle β_m and the groove density N will satisfy the grating equation.

$$\sin\beta_m - \sin\theta = Nm\lambda\,. \tag{2}$$

The incident angle θ is the algebraic value of the incident light direction and the grating orientation if the azimuth angle $\gamma = 0$. In the test system, the incident light is parallel to the z axis, so grating orientation α satisfies $\alpha = \theta$. Here +1 and -1 are the diffraction orders, and β_1, β_{-1} are the diffraction angles corresponding to +1, -1, respectively. They meet Equation (3).

$$\begin{aligned} &\cos(\beta_1-\alpha) = t\,, \\ &\cos(\alpha-\beta_{-1}) = l\,, \\ &\sin\beta_1 - \sin\alpha = N\lambda\,, \\ &\sin\beta_{-1} - \sin\alpha = -N\lambda\,. \end{aligned} \tag{3}$$

In data processing of the test system, the position of six points in step 2 are measured, so the cosine of internal angles t and l are obtained. Then grating orientation α and the grating groove density N can be solved according to Equation (3). The height of the grating investigated point relative to the reference plane which denoted as H is based on the geometric relationships. They can be expressed as

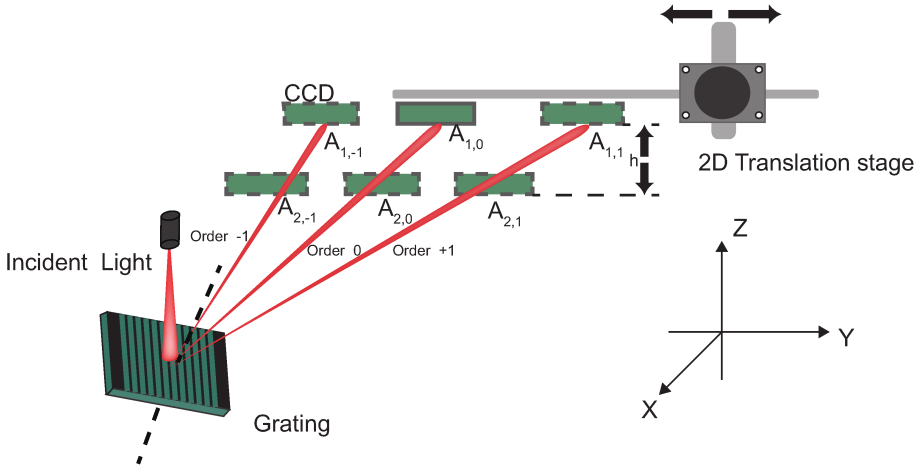

Fig. 1 Sketch of grating measurement system.

Equation (4).

$$\tan\alpha = \frac{\sqrt{1-t^2}-\sqrt{1-l^2}}{(2-t-l)}\,,$$
$$N = \frac{1}{\lambda}\frac{(1-t)\sqrt{1-l^2}+(1-l)\sqrt{1-t^2}}{\sqrt{(2-t-l)^2+\left(\sqrt{1-t^2}-\sqrt{1-l^2}\right)^2}}\,, \quad (4)$$
$$H = h_2 - \frac{y_{21}-y_{20}}{y_{11}-y_{10}-y_{21}+y_{20}}h\,.$$

Equation (4) shows the grating parameters including grating groove density as well as grating position and orientation are constructed simultaneously. The method measures the internal angles between the 0-order and +1,−1-order diffraction lights at one standard wavelength, then grating parameters are obtained according to the grating equation. The measurement principle of transmission grating is similar to the reflection grating. To obtain the groove density distribution of the entire grating, the above steps can be repeated at different positions on the grating point by point. Arbitrary grating surface profile with varied groove density distribution or even mosaic of a group of gratings could be measured by the proposed system.

3 MEASUREMENT UNCERTAINTY

3.1 Measurement Uncertainty of Error Sources

In the method, the measurement uncertainty depends on the measurement error of ray hit point relative positions. Here, a grating in a spectrometer is taken as example. The plane grating works in an incident angle of 4° with constant groove density 333 line mm^{-1}.

The measurement employs a single wavelength laser beam with fixed direction and grating under test keeps stationary. The laser wavelength error, laser spot geometry, the grating surface and groove density variation in the spot can be ignored for constant groove density plane gratings. The plane grating could be aligned and the collimation angle could be identified, so the collimation error is not considered.

Therefore, measurement uncertainty is only from linear guides and the image centroid algorithm which will affect measurement error of the ray hit point. Table 1 lists various error sources. Here, the Monte Carlo method is used to simulate the error sources. Firstly, random numbers are generated and added them to the coordinates of the six points. Secondly, the measurement value are solved according to Equation (4). Thirdly, the measurement uncertainty is calculated by averaging absolute value of each measurement error.

Take example of 2D translation stage horizontal positioning error, which is ±20μm, we generate random number e with expectation $\mu = 0$ and standard deviation $\sigma = 6.67$μm. That is $e \sim N(0, 6.67^2)$, according to the "3σ" principle, the probability of e between -20 μm and 20 μm is 99.7%, the generated random number e is used to simulate the positioning error and added to the nominal value as the measurement value, and grating parameters can be calculated according to Equation (4), and the measurement uncertainty can be calculated. The random number e is generated for 50 000 times. Expectation of absolute measurement error is solved by repeating the previous actions. Since the Monte Carlo method is a statistical simulation method, the random numbers generated in PC are pseudo-random numbers. Simulation results may vary at different time. The simulation results show that the measurement uncertainty of the grating density ($\Delta N/N$) and orientation are 7.52×10^{-5} and 1.12×10^{-2}. The grating position measurement error is 3.45×10^{-2}. Table 1 lists the uncertainty of grating parameters with the distance between the two CCD surfaces(h) is 500 mm. The results show high accuracy in grating parameters identification.

Direction of diffracted rays is measured by intersecting two parallel planes in the simulation. Least square

Table 1 Uncertainty of the Parameters

	Source of error	Uncertainty of the grating groove density $\Delta N/N$	Uncertainty of the grating normal $\Delta\alpha/\alpha$	Measurement error of the grating position (mm)
Centroid positioning error	Detecting the centroid of the light spot error (0.004 mm)	1.50×10^{-5}	2.20×10^{-3}	6.90×10^{-3}
2D translation stage positioning error	Horizontal direction (0.02 mm)	7.52×10^{-5}	1.12×10^{-2}	3.45×10^{-2}
	Vertical direction (0.02 mm)	6.55×10^{-6}	1.10×10^{-3}	1.42×10^{-4}
2D translation stage orientation error	Horizontality (60″)	6.09×10^{-5}	1.20×10^{-3}	4.92×10^{-4}
	Verticality (60″)	7.72×10^{-7}	7.90×10^{-3}	$< 10^{-4}$
Total		9.81×10^{-5}	1.40×10^{-2}	3.52×10^{-2}

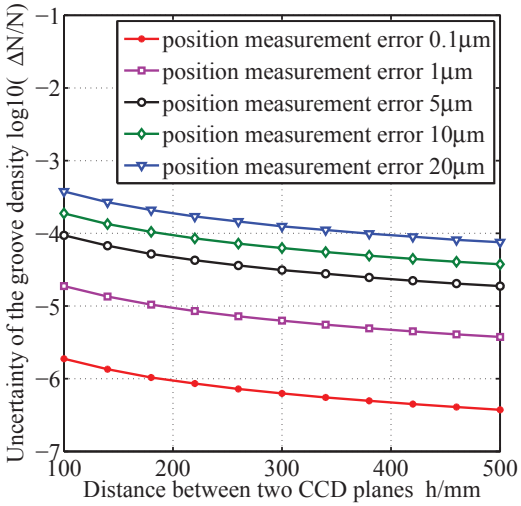

Fig. 2 Uncertainty of groove density with distance between two CCD planes for different positioning accuracy.

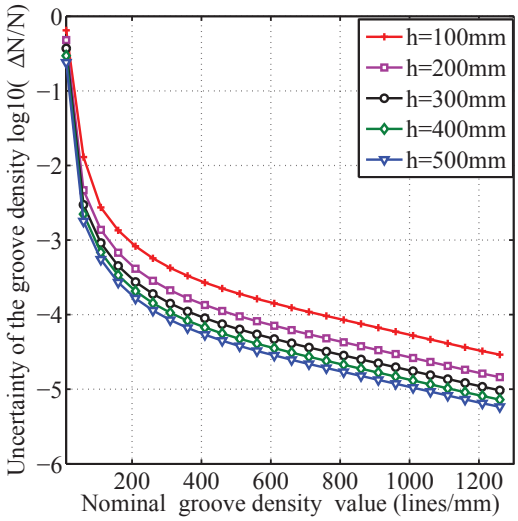

Fig. 3 Grating groove density and measurement uncertainty for different distance h.

method may be used to reduce uncertainty if the diffracted rays are measured among multiple planes.

3.2 Accuracy Dependency on Main Configuration Parameters

Not only the test system error, but also configuration parameters affect grating parameters constructing accuracy. The accuracy dependency on main configuration parameters are evaluated in this section. The groove density identification accuracy dependency is discussed in this section because it reflects the accuracy of the whole test system to a certain extent.

3.2.1 Groove density identification accuracy with respect to distance between two planes

The following numerical simulation shows the relationship between the distance between two planes and the measurement accuracy. Here, the Monte Carlo method is used to simulate the measurement error. The simulated measurement error of ray hit point position are 0.1 μm, 1 μm, 5 μm, 10 μm and 20 μm while the distance(h) between the two different parallel planes changes from 10 cm to 50 cm. The uncertainty of groove density ($\Delta N/N$) is shown in Figure 2. As seen in Figure 2, the accuracy of the grating groove density measurement increases while the distance between the two different parallel planes increases. Therefore, the distance between the two different parallel planes should be as large as possible if technical conditions allow.

3.2.2 Groove density identification accuracy and nominal groove density value

The following numerical simulation shows groove density measurement accuracy with respect to nominal groove density value. The Monte Carlo method is again employed to simulate the ray hit point position error and it is ±20μm. It is assumed that any groove density can be measured here. The uncertainty of groove density ($\Delta N/N$) is shown in Figure 3, with the distance between the two different parallel planes (h) changes from 10 cm to 50 cm and

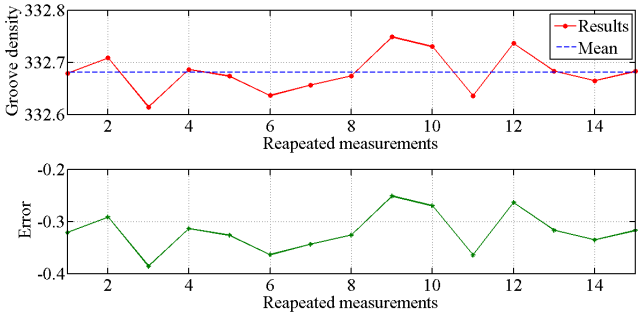

Fig. 4 Measurement results at the same point.

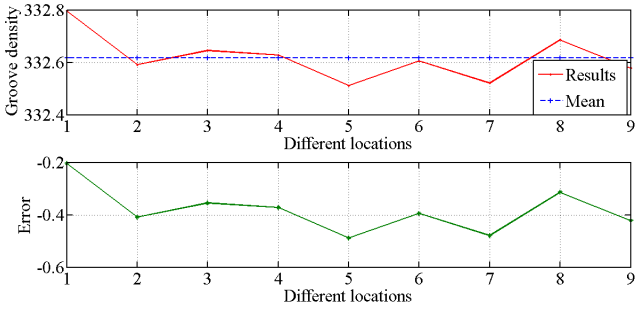

Fig. 5 Measurement results at different locations.

grating groove density changes from 10 lines mm^{-1} to 1260 lines mm^{-1}.

Overall, the accuracy of the groove density increases while the distance between the two different parallel planes (h) increases. It can be known that when h is 500 mm, for a grating with groove density greater than 310 lines mm-1, $\Delta N/N$ is less than 10^{-4}, which shows high measurement accuracy.

4 A VERIFICATION STUDY

The most simple verification testing without calibrating is carried out to verify the validity of the principle and measure a planar transmission grating with a nominal groove density of 333 lines mm^{-1}. A 632.81 nm wavelength high-stability He–Ne laser is used as a standard wavelength. The pixel size of the CCD is 4.45 μm. To carry out the testing system simplicity, the dispersion direction of the grating is vertically, the 2D translation stage shifts back and forth and stays on two parallel planes which is perpendicular to the optical axis. First, obtaining 1, 0, –1-order diffracted rays by shifting the 2D translation stage up and down (the dispersion direction) in one plane. Then the 2D translation stage advances 50 mm along the optical axis to the second plane, and the three diffracted rays are obtained again. Through data processing and Equations (1)–(4), the grating parameters are obtained.

To evaluate the accuracy of testing system components is the first step after establishing the verification system. In order to evaluate the accuracy of the centroid positioning, the centroid detection is performed on the same point. In theory, the coordinate of the centroid remains unchanged. Due to the uncertainty of the centroid positioning, the result is different. The RMS of the centroid detection algorithm is calculated and it is less than 0.3 pixels, which indicates that the algorithm has high accuracy and stability. It is applied to the measurement.

The CCD measures the same point by moving the 2D translation stage up and down to evaluate the positioning accuracy of linear guide in the vertical direction. Measuring the same point by moving the 2D translation stage up and down vertically 0.5 mm each time. Theoretically, this point is fixed, and its position deviation in CCD should be 0.5 mm. Due to the positioning error of the translation stage and centroid algorithm, the deviation of the centroid should not be 0.5 mm. The mean value of vertical positioning error is –0.1777 μm, and the standard deviation is 3.5077 μm. According to the "3σ" principle, it can be seen that the probability of the positioning error in $(-10.7008, 8.5947)$ is 99.7%.

To evaluate the tilt angle of the translation stage relative to the optical axis, 0-order diffracted light is measured by CCD with moving it back and forth along the optical axis. The centroid position of the 0-order diffracted light on it remains unchanged theoretically. Due to the translation stage tilt, the position of the 0-order diffracted light is shifting. Then the translation stage tilt angle can be estimated. According to linear fitting results, the slopes of two directions are -0.02308 and 0.001598. It can be concluded that the 2D translation stage has a certain tilt angle with respect to the optical axis. The angles in two directions are 1.3221° and 0.0911°.

The accuracy of each component in the test system is evaluated. The angle between the translation stage and the optical axis is planned to be compensated by data processing. The verification test system is applied to the grating parameters test.

Figure 4 shows 15 measurements of the same investigated point in the grating. The average of the result is 332.6806 lines /mm, and the uncertainty of groove density ($\Delta N/N$) is 9.5916×10^{-4}. The RMS of the measurement result is 0.0368 lines mm^{-1}. Figure 5 shows the measurement result at nine different investigated points in the grating. The average of the result is 332.6183 lines mm^{-1}. The RMS of the measurement result is 0.0818 lines mm^{-1}. The measurement results demonstrate that this method has good reproducibility.

5 MEASURABLE GRATING GROOVE DENSITY BY THE METHOD

Due to the limited travel of the 2D translation stage, it might not cover all rays extent by moving it, which is the main factor that limits the measurable grating parameters.

Obviously, the method is applicable when the detector can obtain the –1, 0, and +1-order diffracted rays by moving the linear guide. According to the grating equation, the angle between the –1-order and the +1-order diffracted light is small when the groove density is small and vice versa. If the angle between the –1-order and the +1-order diffracted light is large, the distance between the –1-order and the +1-order diffracted light on plane is longer than linear guide travel distance, the grating parameters cannot be measured. The measurable angle between diffracted lights limited by linear motion travel distance is discussed in Section 5.1. Measurable grating groove density of the method is analyzed in Section 5.2. An improved method to broaden the measurable groove density is proposed in Section 5.3.

5.1 Measurable Diffraction Angles Limited by Linear Motion

The angles between the –1-order and +1-order diffracted rays which are limited by the test system is discussed here. A simplified system is shown in Figure 6 where the two planes show the different CCD locations and the position P shows the investigated point in grating in Figure 1. The two ends of the horizontal translation stage on the first plane are denoted as A and B. Our goal is to find a certain position P below the second surface so that the angle between PA and PB, which is denoted as ψ, is the largest. If the angle between the –1-order diffracted light and the +1-order diffracted light exceeds ψ for a certain grating groove density, this grating groove density is not measurable in the method.

But there is no definite expression for ψ. We find a upper limit of ψ. Obviously, when the point P is located on the second surface (point O), and satisfies OA = OB, a corresponding maximum angle $\psi_{\max}$ is reached. As shown in Figure 6, the maximum angle $\psi_{\max}$ can be calculated. $\psi_{\max}$ is larger than ψ.

The angle between the –1-order and the +1-order diffracted light is $\psi_{\max}$ when the groove density is a certain value in the method. The corresponding value is the upper limit of maximum measurable groove density.

The distance between two CCD planes is $h = ks$, where k is the rate and s is the 2D translation stage horizontal travel distance. It is easy to know that, as shown in Figure 6, the maximum value $\psi_{\max}$ satisfies $\tan\psi_{\max} = 4k/(4k^2-1)$. It is obvious that $0° < \psi_{\max} < 180°$. When $k < 0.5$ and $0.5 < k < 1$, $\psi_{\max}$ is an obtuse angle and acute angle, respectively. When $k = 0.5$, $\psi_{\max} = 90°$.

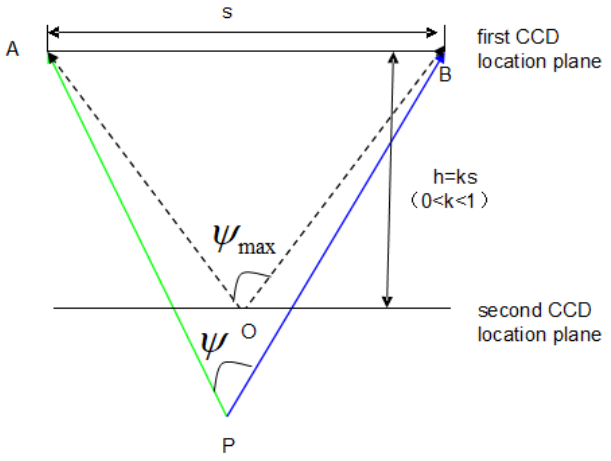

Fig. 6 The maximum angle between –1-order and +1-order limited by linear motion.

5.2 Measurable Grating Groove Density of the Method

To analyze the measurable grating groove density of the method, it is guaranteed that the angle between –1-order and +1-order diffracted light is less than $\psi_{\max}$ solved in Section 5.1. The measurable grating groove density of the method is discussed here. The grating groove density is measurable when two conditions are met: Firstly, the output contains +1-order, –1-order and 0-order diffracted lights. Secondly, the angle between –1-order and +1-order diffracted light is smaller than $\psi_{\max}$ solved in 5.1.

For the first condition, Equation (5) should be satisfying

$$\begin{aligned} |\sin\beta_1| &= |N\lambda + \sin\alpha| \le 1\,, \\ |\sin\beta_{-1}| &= |-N\lambda + \sin\alpha| \le 1\,. \end{aligned} \tag{5}$$

The incident angle in Equation (5) is related to the specific application. There is

$$N \le \frac{1-|\sin\alpha|}{\lambda}\,. \tag{6}$$

For the second condition, there is $\beta_1 - \beta_{-1} < \psi_{\max}$. According to the grating equation, there is

$$\begin{aligned} 2N\lambda &= \sin\beta_1 - \sin\beta_{-1} \\ &= \sin(\beta_1-\beta_{-1})\cos\beta_{-1} \\ &\quad + [\cos(\beta_1-\beta_{-1})-1]\sin\beta_{-1} \\ &\le \sqrt{2-2\cos(\beta_1-\beta_{-1})} \\ &\le \sqrt{2-2\cos\psi_{\max}} \\ &= \sqrt{2-\frac{2(4k^2-1)}{\sqrt{16k^2+(4k^2-1)^2}}}\,. \end{aligned} \tag{7, 8}$$

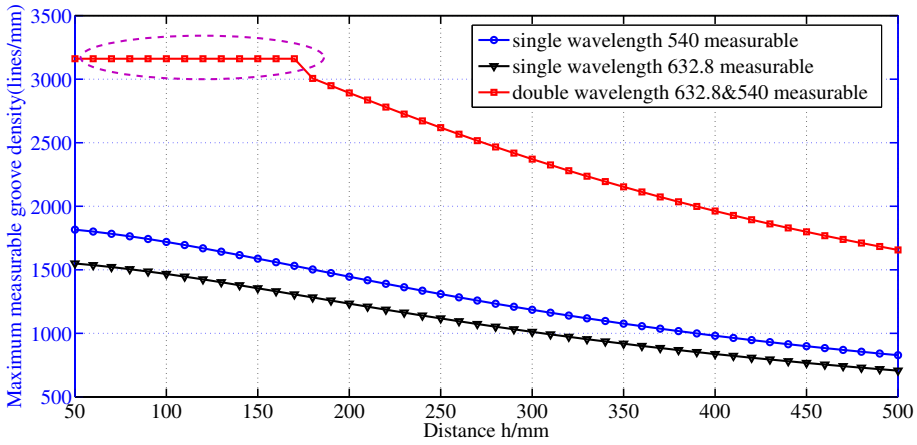

Fig. 7 The measurable groove density and distance.

According to Equations. (6) and (7), the maximum grating groove density is denoted as $N_{\max}$, there is

$$N_{\max} < \min\left(\frac{\sqrt{2-\frac{2(4k^2-1)}{\sqrt{16k^2+(4k^2-1)^2}}}}{2\lambda}, \frac{1-|\sin\alpha|}{\lambda}\right). \tag{9}$$

For example, when $k = 0.5$, $\psi_{\max} = 90°$. It means the measurable angle between –1-order and +1-order diffracted rays can approach 90° infinitely in the test system. If the angle between the –1-order and the +1-order diffracted lights exceeds 90° for a certain grating groove density, the grating cannot be measured by the test system. Here, we imagine a case when the angle between the –1-order and the +1-order diffracted light is 90°, and the corresponding groove density is the largest. When the incident angle is 0°, the +1-order diffraction angle is 45°, and the –1-order diffraction angle is −45°, in this case, the corresponding groove density is the largest, it is $N = \sqrt{2}/2\lambda$, which is in accordance with Equation (9). Firstly, the angle between –1-order and +1-order diffracted light is less than 90° when $k = 0.5$ in practice. Secondly, achieving the maximum measurable groove density is related to the grating working conditions. Therefore, Equation (9) is the upper limit of the measurable groove density.

Equation (9) shows that shorter probing wavelength can widen the measurable groove density. The maximum measurable grating groove density is related to the specific application. Reducing the distance h which means k decreasing can also increase measurable groove density. Due to the limitations of the experimental system, the distance between two CCD planes cannot be decreasing arbitrarily. In addition, it is known from 3.2 that the larger distance h, the higher the measurement accuracy within a certain range. Equation (9) also shows that the maximum grating groove density with incident angle α is the same as $-\alpha$ in the method.

5.3 An Improved Method to Broaden the Measurable Groove Density

The method detects –1, 0 and +1-order diffracted rays of a wavelength. The limiting factor that restricts the measurable groove density is angle between the –1-order and +1-order diffracted light should less than $\psi_{\max}$. In order to widen the measurement range, double-wavelength method can be used. In the double-wavelength method, 0 and +1-order diffracted rays are detected, so the angle between the 0-order and +1-order diffracted light should less than $\psi_{\max}$.

The Littrow condition is satisfied when the direction of incident light is the same as diffracted light. For wavelength λ, the incident angle α will satisfy $2\sin\alpha = \lambda N$.

For the two laser beams with the wavelengths λ_1 and λ_2 incident on the grating after they combines. We assume $\lambda_1 < \lambda_2$ here. The grating is mounted in Littrow configuration in wavelength λ_2. The grating groove density can be measured.

The grating incident angle α, the +1-order diffraction angle β_1 of λ_1 meet Equation (10). The angle between the +1-order and the 0-order diffracted light φ can be obtained from the coordinates of four points in two CCD surfaces. The groove density N is measured.

$$\begin{aligned} &2\sin\alpha = \lambda_2 N\,, \\ &\sin\beta_1 - \sin\alpha = \lambda_1 N\,, \\ &\beta_1 - \alpha = \varphi\,. \end{aligned} \tag{10}$$

At this time, φ is smaller than $\psi_{\max}$ as discussed in 5.1. There is

$$N_{\max} < \min\left(\sqrt{2 - \frac{2(4k^2-1)}{\sqrt{16k^2+(4k^2-1)^2}}}/\lambda_1, \frac{2}{\lambda_2}\right) \tag{11}$$

For the single wavelength and the double-wavelength method with the detection wavelength 632.8 nm and 540 nm, $s = 500$ mm, the distance between two CCD planes (h), the maximum measurable groove density are shown in Figure 7.

It can be known from Figure 7 that as the distance between two different parallel planes (h) becomes larger, the maximum measurable groove density becomes smaller, but at the same time the measurement accuracy improves based on 3.2. For single-wavelength, shorter probing wavelength can expand measurable groove density. For double-wavelength method, when h is less than a certain value, the limiting factor of the measurement range is that the diffracted lights can be observed as shown in the circle in Figure 7. According to Equation (9), Equation (11) and Figure 7, the measurable groove density of double-wavelength is nearly twice as the single-wavelength.

6 CONCLUSION

A simple method achieving high precision and wide applicable range for grating multiple parameters identification is proposed in this paper. The groove density, grating position and orientation could be identified simultaneously for transmission gratings or reflection gratings. Arbitrary grating surface profile with varied groove density distribution or even mosaic of a group of various gratings could be measured by the proposed system. Based on the Monte Carlo method, various error sources are simulated, and their effects on measurement accuracy are analyzed. The simulation results show that it has high accuracy. The accuracy dependency on main configuration parameters are further evaluated. A double-wavelength method is introduced to expand the measurement range.

Acknowledgements This work was supported by the National Natural Science Foundation of China (Grant Nos. 11927804 and 11873013).

References

Binkele, T., Hilbig, D., Ceyhan, U., Gutierrez, G., & Fleischmann, F. 2018a, Experimental Ray Tracing C from simulation to reality, in Frontiers in Optics / Laser Science, paper JW4A.8, https://doi.org/10.1364/FIO.2018.JW4A.8

Binkele, T., Hilbig, D., Fleischmann, F., & Henning, T. 2018b, in Optical Instrument Science, Technology, and Applications, SPIE Conference Series, 10695, 106950F

Binkele, T., Vassmer, D., Hilbig, D., Fleischmann, F., & Henning, T. 2017, in Society of Photo-optical Instrumentation Engineers (SPIE) Conference Series, 10448, 1044816

Ceyhan, U., Henning, T., Fleischmann, F., Hilbig, D., & Knipp, D. 2011, in Optical Measurement Systems for Industrial Inspection VII, SPIE Conference Series, 8082, 80821K

Du, L., Du, X., & Wang, Q. 2016, AIP Conference Proceedings 1741, 040039

Gutierrez, G., Hilbig, D., Fleischmann, F., & Henning, T. 2017, in Society of Photo-Optical Instrumentation Engineers (SPIE) Conference Series, 10110, 101100E

Hiroyuki, I., & Tomohiro, T. 2014, Applied Optics, 53, 5290-3, *doi: 10.1364/AO.53.005290*

Hu, Z., Liu, Z., & Wang, Q. 2004, Review of Scientific Instruments, 75, 4419

Häusler, G., & Schneider, G. 1988, Applied Optics, 27, 5160

Liu, B., Wang, Q., Xu, X., & Fu, S. 2006, Review of Scientific Instruments, 77, 046106

Oster, G., Wasserman, M., & Zwerling, C. 1964, Josa, 54, 169

Sharma, D., Sharma, R., Dua, S., & Ojha, V. N. 2012, 2nd National Conference on Advances in Metrology(AdMet), 1, https://www.researchgate.net/publication/262374480_Pitch_Measurements_of_1D2D_Gratings_using_Optical_Profiler_and_comparison_with_SEM_AFM

Sheng, B., Chen, G., Huang, Y., & Luo, L. 2017, Review of Scientific Instruments, 88, 106102

Sheng, B., Chen, G., Huang, Y., & Luo, L. 2018, Appl Opt, 57, 2514

Tai, H. Y., Eom, C. I., Chung, M. S., & Hong, J. K. 1999, Optics Letters, 24, 107

Wang, Q., Liu, Z., Chen, H., et al. 2015, Review of Scientific Instruments, 86, 023109